Supercritical fluid deposition of Ru nanoparticles into SiO_2 SBA-15 as a sustainable method to prepare selective hydrogenation catalysts

J. Morère[a], M.J. Torralvo[b], C. Pando[a], J.A.R. Renuncio[a] and A. Cabañas*[a]

[a] Department of Physical Chemistry I, Universidad Complutense de Madrid, 28040 Madrid. SPAIN

[b] Department of Inorganic Chemistry I, Universidad Complutense de Madrid, 28040 Madrid. SPAIN

*Send correspondence to:

Prof. Albertina Cabañas

Department of Physical Chemistry I

Universidad Complutense de Madrid

Ciudad Universitaria s/n, 28040 Madrid SPAIN

Tlf: 34 + 91 3945225 Fax: 34 + 91 3944135

e-mail: a.cabanas@quim.ucm.es

ABSTRACT

Ru nanoparticles were successfully deposited into mesoporous SiO_2 SBA-15 using supercritical CO_2 ($scCO_2$). The use of $scCO_2$ favoured the metal dispersion and Ru nanoparticles uniformly distributed throughout the support were obtained. Different precursors and methodologies were employed: impregnation with $Ru(tmhd)_2(COD)$ in $scCO_2$ at 80 ºC and 13.5 and 19.3 MPa and further reduction in H_2/N_2 at 400 ºC at low pressure, reactive deposition of $Ru(tmhd)_2(COD)$ with H_2 in $scCO_2$ at 150 ºC and reactive deposition of $RuCl_3 \cdot xH_2O$ with ethanol in $scCO_2$ at 150 and 200 ºC. The size of the particles was limited in one dimension by the pore size of the support. The metal loading varied with the methodology and experimental conditions from 0.9 to 7.4% Ru mol. These materials exhibited remarkable catalytic activity. The Ru/SiO_2 SBA-15 materials prepared by reactive deposition with H_2 in $scCO_2$ were selective catalysts for the hydrogenation reactions of benzene and limonene, allowing the production of partly hydrogenated hydrocarbons that may serve as building blocks for more complex chemicals. $scCO_2$ is shown to be a green solvent that allows the preparation of efficient heterogeneous catalysts to design sustainable processes. Furthermore, in the hydrogenation of limonene, $scCO_2$ was also used as the solvent.

1. Introduction

Ruthenium catalysts have been widely used in heterogeneous catalysis particularly in hydrogenation reactions. In comparison to other traditional metal catalysts such as Pd, Pt, or Rh, Ru has been shown to perform better in selective hydrogenation reactions.[1] Ru catalysts have been used for the partial hydrogenation of aromatics [2, 3] and the selective hydrogenation of carbonyl groups in the vicinity of either a double bond or an aromatic ring.[1] These are very important processes from both environmental and economic reasons. For example, the partial hydrogenation of benzene to cyclohexene provides a more efficient and low cost route for the production of chemical intermediates for nylon.[4] Other interesting example of the use of Ru catalysts is the selective hydrogenation of terpenes such as α and β pinene, 1,8-cineol, citral and limonene. These compounds can be extracted from renewable sources and are very cheap precursors of fragrances, flavours, drugs and agrochemicals. Partly hydrogenated terpenes are interesting building blocks for fine chemicals.[5]

Ruthenium catalysts have been supported on amorphous alumina, silica, titania or active charcoal,[6] mesoporous silica materials MCM-41, SBA-15 and HMS,[7] KL zeolite,[8] porous metal-organic frameworks,[9] carbon nanotubes, ZnO,[4] ZrO_2,[8] and montmorillonite,[10] among others. The activity and selectivity of the catalyst depend on the metal concentration, metal particle size and its distribution, as well as on the chemical nature of the support, its morphology and the metal-support interactions. In principle, the better the dispersion, the higher the activity of the support.

The synthesis of supported metal nanoparticles on solid porous supports and the different preparations routes have been recently reviewed.[11] Among the different preparation routes, the use of supercritical fluids deserved especial attention.

Zhang and Erkey have reviewed the preparation of supported metallic nanoparticles using supercritical fluids.[12, 13] Although in principle any supercritical fluid can be used, most experiments have been performed using CO_2 (T_c= 31 ºC and P_c= 7.4 MPa). The use of $scCO_2$ presents a number of advantages in materials processing and synthesis.[14] Supercritical CO_2 ($scCO_2$) has densities intermediate between those of liquids and gases, but transport properties (diffusivity and viscosity) similar to gases. This combination of properties makes possible to introduce precursors dissolved in the supercritical fluid inside highly porous inorganic substrates.[15, 16] On the other hand, the high solubility of $scCO_2$ in amorphous polymers leads to swelling of the polymer and a decrease in its glass transition temperature and enhances the chain mobility of the polymers, making also possible the incorporation of materials within polymeric substrates.[17] Furthermore, CO_2 properties can be tuned with small changes of pressure and temperature, and the characteristics of the composite material can be controlled in the same way. [18] From an environmental point of view, CO_2 is considered a green solvent because it has moderate critical parameters, it is cheap, non-toxic, non-flammable and can be recycled. CO_2 is a gas at ambient pressure and can be eliminated easily by simple depressurization without leaving any residue.

The Supercritical Fluid Deposition technique (SFD) was originally proposed by Watkins et al. [19, 20] The method involves the dissolution of a metal precursor in the supercritical fluid and its adsorption onto a given support (planar or porous). Then the metal precursor is decomposed, either in the supercritical fluid (by addition of a reducing agent such as H_2 or an alcohol, or simply by heat treatment), or after depressurization of the system under controlled atmosphere, yielding the metal or metal oxide/support composite materials. By controlling the reaction conditions, films or nanoparticles can be deposited into planar and porous substrates.

In this paper we study the deposition of metal nanoparticles into a highly porous support, mesoporous silica SBA-15. Traditional preparative methods in liquid solution often yield inhomogeneous materials due to the high surface tension of most liquids, the slow diffusion of the metal precursor within the support pores and the potential damage of the support during the drying process. On the other hand, gas based processes such as Chemical Vapour Deposition (CVD) tend to yield non uniform materials mainly because of volatility constrains, which lead to mass transport-limited conditions and poor step coverage. The use of $scCO_2$ in metallization processes presents several advantages over the conventional techniques. Beside the environmental benefits, the transport properties of $scCO_2$ favour the penetration of $scCO_2$ and its solutions into nanostructures and nanopores. In this way, metal nanoparticles can be introduced within the micro and mesopores of different substrates in a much more efficient way than the conventional processes in both liquid and gas phases.

The deposition of Ru onto different porous and planar supports using $scCO_2$ has been pursued because of their numerous applications in microelectronics, catalysis and electrochemistry.[21-24] In these studies, different precursors and methodologies have been used. All these methods require the solubilisation of the metal precursor in the supercritical fluid mixture. The particular choice of precursor and fluid determines the solubilisation temperature and pressure used. Then, if the decomposition of the precursor is carried out under supercritical conditions, addition of a reducing agent and/or increase of the temperature and pressure are required. The decomposition of the precursor can be also carried out after depressurization of the reactor by thermal treatment of the impregnated support in a controlled atmosphere.

Ru thin films were successfully deposited onto silicon wafers by the H_2 reduction of bis(2,2,6,6-tetramethyl-3,5-heptanedionato)(1,5-octadiene) ruthenium (II)

[$Ru(tmhd)_2(COD)$] [22, 25] and bis-cyclopentadienylruthenium [$Ru(Cp)_2$][21, 26] at temperatures between 250-350 ºC in $scCO_2$. Similarly, Ru nanoparticles were deposited onto carbon nanotubes (CNT) by the H_2 reduction of ruthenium acetylacetonate [$Ru(acac)_2$] in pure $scCO_2$ at 250 ºC,[27] and from $RuCl_3 \cdot 3H_2O$ in supercritical CO_2-methanol solutions at 200 ºC.[28] Ru nanoparticles were also immobilized into metal-organic framework nanorods from $RuCl_3 \cdot 3H_2O$ in supercritical CO_2-methanol solutions at 200 ºC.[29] The alcohol acted as cosolvent as well as reductant. The same precursor was used to deposited Ru nanoparticles onto CNTs in supercritical methanol at 300 ºC [30] and in supercritical water at 400-450 ºC [31] and to produce Ru/graphene composites in supercritical water at 400 ºC.[32] Similarly, Yen et al. used a hybrid approach and impregnated a mesoporosus SiO_2 SBA-15 with a solution of $Ru(acac)_2$ in THF followed by drying under vacuum and H_2 reduction in $scCO_2$ at 200 ºC.[33] In all these examples, the precursor reduction was carried out at supercritical conditions.

Others have followed a different approach and used $scCO_2$ as the solvent to impregnate the metal precursor into the support. The precursor is then decomposed after depressurization of the system by thermal treatment under a reducing atmosphere. In this way, $Ru(acac)_3$ and $Ru(tmhd)_2(COD)$ dissolved in $scCO_2$ were impregnated into carbon aerogels (CA) at 80 ºC and then reduced in N_2 at low pressure.[23] The thermodynamic and kinetics of adsorption of $Ru(tmhd)_2(COD)$ on CA were also reported.[34] Using the same technique, polydimethylsilosane (PDMS) films were also impregnated at 40 ºC with the same precursor and further decomposed in N_2 atmosphere.[35] A similar approach was used to produce silica aerogel-Ru composites using $Ru(acac)_3$.[36] This precursor was also used to deposit Ru onto nanoporous silica FSM-16.[37] The support was impregnated with $Ru(acac)_3$ dissolved in $scCO_2$ at 150 ºC using acetone as the cosolvent, followed by thermal reduction at low pressure in H_2/N_2.

$RuCl_3 \cdot 3H_2O$ and $Ru(acac)_2$ were also used in combination with ethanol to impregnate activated carbon at 45 ºC and 10.0 MPa. The impregnated material was reduced in H_2/N_2 at 350 ºC at low pressure.[38] Similarly, CNT were impregnated with $RuCl_3 \cdot 3H_2O$ at 140 ºC and 8.0 MPa in a supercritical CO_2–ethanol solution and further reduced in H_2 at 400 ºC at low pressure.[39]

Although a relatively large number of publications on the deposition of Ru nanoparticles in supercritical fluids has been published, there is not a comprehensive study comparing the different reaction routes and precursors. In this work, we carry out this comparative study and perform impregnation, H_2–reduction and alcohol reduction experiments using $Ru(tmhd)_2(COD)$ and $RuCl_3 \cdot 3H_2O$ on mesoporous SiO_2 SBA-15 as support. The aim of this work is to elucidate the role that the different variables have on the final material and hopefully serve as a selection guide to deposit Ru from supercritical solutions.

Furthermore, we demonstrate that these materials serve as selective catalysts in the hydrogenation reactions of benzene and limonene. In the hydrogenation of limonene, the reaction was performed in $scCO_2$. Due to its tuneable solvent properties and its green nature, $scCO_2$ is a very attractive medium for chemical reactions.[40-42] $scCO_2$ and H_2 are fully miscible[43] and limonene can be dissolved in such a mixture at moderate temperatures and pressures. Bogel-Lukasik *et al.* studied the phase behaviour of the ternary system CO_2/H_2/limonene and shown that selectivity in the hydrogenation of limonene in $scCO_2$ can be tuned by changing the pressure.[44] These authors have also studied the effect of the catalyst in this reaction and performed experiments using Pt/C, Pd/C and Ru/Al_2O_3 combined with an ionic liquid.[44-46] In this work, the Ru catalysts produced using $scCO_2$ have been tested in the hydrogenation reaction of limonene in CO_2 at supercritical conditions.

2. Experimental

2.1. Materials

Tetraethylorthosilicate (TEOS, 99+% pure), poly(ethylene glycol)-block-poly(propylene glycol)-block-poly(ethylene glycol) (Mw=5800) (PEO-PPO-PEO), dichloromethane (99,99%), hexane (+ 99%), (R)-(+)-limonene (97%), $ZnSO_4 \cdot 7\ H_2O$ and $RuCl_3 \cdot xH_2O$ (+99.98%) were obtained from Sigma-Aldrich. Benzene (>99.5%) was obtained from Panreac and ethanol (+99.8%) was supplied by Scharlau. $Ru(tmhd)_2(COD)$ was provided by Strem chemicals (99%). CO_2 (purity >99.99%) and H_2 (purity >99.999%) were supplied by Air Liquide. 5% H_2/N_2 forming gas was supplied by Contse.

Mesoporous silica SBA-15 was prepared following the procedure described by Zhao *et al.*[47, 48] In a typical experiment, 4.0 g of PEO-PPO-PEO were dissolved in 30 g of water and 120 g of 2 M HCl solution with stirring at 35 ºC. Then 8.5 g of TEOS was added into the solution with stirring at 40ºC for 20 hours. The mixture was aged at 100ºC without stirring for a further 12 hours. The solid residue was filtered, washed with ethanol several times and calcined in air at 550 ºC for 6 hours. Heating rate from room temperature was 1ºC/min.

2.2 Materials preparation

Ru deposition into mesoporous silica SBA-15 was carried out in supercritical CO_2 following three different procedures[‡]: a) impregnation, b) reactive deposition using H_2 and c) reactive deposition using EtOH. $Ru(tmhd)_2(COD)$ and $RuCl_3 \cdot xH_2O$ were used as the metal precursors. The experimental procedure is summarized in Scheme 1.

Most experiments were conducted in a *ca*. 100 mL stirred high-pressure reactor (Autoclave Eng. Inc.) in the batch mode. In the *impregnation experiments*, approximately 150 mg of the support and 70 mg of $Ru(tmhd)_2(COD)$ were loaded into the reactor ($Ru:SiO_2$ molar ratio close to 1:20). The reactor was then heated by a heating jacket

connected to a PDI controller to 80 ºC and was then filled with CO_2 using a high-pressure syringe pump (Isco, Inc. Model 260D) thermostated at the same temperature up to 13.5 or 19.3 MPa. The temperature was measured using a K-type thermocouple. The pressure was measured using a pressure gauge. Impregnation experiments were carried out in $scCO_2$ under stirring for 24 hours. The reactor was then depressurized through a needle valve in 1 hour. The Ru impregnated SiO_2 SBA-15 samples were then decomposed in a tube furnace under N_2/H_2 atmosphere for 5 hours at 400 ºC and atmospheric pressure. Heating rate in both cases was 10 ºC/min.

Reactive deposition experiments using H_2 were carried out on the SiO_2 support using $Ru(tmhd)_2(COD)$. The experiments were conducted in the 100 mL stirred stainless-steel high-pressure reactor previously described in the batch mode. SiO_2 SBA-15 (ca. 150 mg) and $Ru(tmhd)_2(COD)$ (ca. 70 mg) were loaded into the reactor ($Ru:SiO_2$ molar ratio close to 1:20). Excess H_2 (50 fold excess) was added to the reactor using a ca. 30 mL auxiliary cell constructed from Swagelok ¾ inch pipe and filled with 15 bar H_2, by flushing CO_2 from the thermostated Isco high-pressure syringe pump through the auxiliary cell up to a final pressure of 140 bar. System was kept at these conditions for 2 hours for complete dissolution. At these conditions, reduction of the precursor did not take place. To promote the precursor reduction, the temperature was increased at 150 ºC. Reduction was complete in 3 hours and depressurization was carried out through a needle valve in 1 hour. Samples were further extracted to remove unreacted precursor and/or the hydrogenated ligand.

Reactive deposition experiments using EtOH were carried out on the mesoporous SiO_2 using $Ru(tmhd)_2(COD)$ and $RuCl_3 \cdot xH_2O$ as precursors. Approximately 150 mg of the support and 10-20 mg of $RuCl_3 \cdot xH_2O$ or 70 mg of $Ru(tmhd)_2(COD)$ ($Ru:SiO_2$ molar ratio ranging from 1:48 to 1:20) and a small amount of EtOH (10% mol in CO_2) were

loaded into the 100 mL stirred high-pressure reactor. In the $Ru(tmhd)_2(COD)$ experiments the reactor was then heated by the heating jacket to 80 ºC and was filled with CO_2 using the high-pressure syringe pump thermostated at the same temperature to a final pressure of 13.5 MPa. In the $RuCl_3 \cdot xH_2O$ experiments, the reactor was however loaded at 35 ºC and 8.5 MPa. In this case, the temperature was kept low to avoid decomposition. Experiments performed in a view cell previously described [49] showed that $RuCl_3 \cdot xH_2O$ at these conditions is soluble in the 10% $EtOH/CO_2$ mixture but it starts to decomposes at temperatures as low as 60 ºC. In one experiment with $RuCl_3 \cdot xH_2O$, the mass of support was reduced to 50 mg to increase the precursor to support molar ratio to 1:6 but assuring complete precursor solubility. The system was kept under stirring at 35 ºC and 8.5 MPa for 2 hours to promote dissolution of the precursor in the supercritical mixture and its impregnation on the support. Then the reactor was heated at 150-200 ºC for another 2-4 hours for its decomposition. During these experiments the pressure was kept below 30.0 MPa (which is the maximum pressure rating of the equipment) by venting a small amount of the CO_2 solution from 100 ºC. Then, the heater was turned off and the reactor was depressurized through a needle valve in 1 hour.

2.3. Materials characterization

Materials were characterized using transmission electron microscopy (TEM), N_2-adsorption, X-ray diffraction (XRD), thermogravimetric analysis (TGA). Selected samples were studied by X-ray Fluorescence spectrometry (XRF). TEM were carried out on a JEOL JEM 2100 electron microscope working at 200 kV and a JEOL-JEM 3000F electron microscope operating at 300 kV. Both TEM microscopes were equipped with a double tilting (±25º) and Energy-dispersive Detection X-ray analysis (EDX) (Oxford INCA). Samples were dispersed in 1-butanol over copper grids and dried in air. N_2 adsorption/desorption isotherms at 77 K were obtained using a Micromeritics ASAP-

2020. Prior to adsorption measurements, SiO_2 samples were out-gassed at 110 ºC and ~10^{-1} Pa for 6 h. Isotherms were analysed using standard procedures. The BET equation was used for specific surface calculations.[50] The total pore volume was estimated from the amount adsorbed at a relative pressure of 0.995. The pore size distributions were calculated using the Barrett, Joyner and Halenda (BJH) method for a cylindrical pore model [51] corrected by the statistical thickness using the adsorption and desorption branches of the isotherms. The actual pore size was estimated from the adsorption branch.

Wide angle XRD patterns of the composite materials were collected using a X´PERT MPD diffractometer with Cu K-α radiation on the conventional Bragg-Brentano geometry at 2θ values between 10 and 80º. TGA of the impregnated supports were obtained on a Perkin-Elmer Pyris 1 at a heating rate of 10 ºC/min in N2 flow (100 cm^3/min). Ru content on selected samples was determined by XRF. A PANalytical Wavelength dispersive X-ray fluorescence spectrometer (4 kW) was used placing the samples in plastic holders in powder form. Quantification was performed using internal standards of the instrument.

2.4. Catalytic tests

Catalytic tests of selected materials were performed.[‡] The catalytic hydrogenations of benzene (Scheme 2) and limonene (Scheme 3) were chosen as model reactions. In both reactions the intermediate hydrogenated compounds are difficult to obtain using other conventional hydrogenation catalysts such as Pt and Pd.

The hydrogenation of benzene was carried out using a ca. 10 mL high-pressure batch reactor constructed from Swagelok ¾ inch stainless steel pipe. The reactor was connected to a pressure transducer and provided with a Swagelok safety valve. Two

different procedures were used: hydrogenation without solvent in pure H_2 and hydrogenation in aqueous $ZnSO_4$ solution.

For the hydrogenation of benzene in pure H_2, a given amount of Ru-catalyst (30-50 mg, depending on the catalyst) and 2 mL of benzene were charged into the reactor along with a stirring bar. The reactor was sealed and purged with H_2 at low pressure several times. The reactor was heated at 40 ºC using a Teflon heating tape (Omegalux SRT051-040) connected to a PID controller (Microomega, model CN77322) using a type J calibrated thermocouple attached to the reactor wall. To start the reaction, H_2 was added to the reactor up to a pressure of 2.0 MPa and kept at these conditions under stirring for a given time (15-40 minutes). During the catalytic test, the reactor was connected to a H_2 reservoir to keep pressure constant. The reaction was terminated by removing the heating tape and immersing the reactor into an ice bath. Then the system was quickly depressurised. In other experiments a 60 mL custom made high-pressure stainless steel reactor heated with a custom made furnace was employed following the same procedure.

In order to improve selectivity to cyclohexene, the hydrogenation of benzene in aqueous $ZnSO_4$ solutions was also tried. It has been reported that this salt is chemisorbed on the surface of the Ru catalyst increasing the hydrophilicity of the catalyst and that, in the presence of a water layer, induces desorption of the partial hydrogenated product before complete reduction, improving selectivity towards cyclohexene.[52] The procedure used in this case is described next. A given amount of Ru-catalyst (30-50 mg, depending on the catalyst), along with 1.0 mL of benzene and 2.0 mL of a 0.400 M $ZnSO_4$ solution were charged into the 60 mL high-pressure stainless steel reactor along with a stirring bar. The reactor was sealed and purged with low pressure H_2 several times. Then the reactor was heated to 150 ºC with a custom made furnace connected to a PID controller (Microomega, model CN77322) using a type J calibrated thermocouple attached to the

reactor wall. At this temperature, H_2 was added to the reactor until a pressure equal to 4.0 MPa. Reaction was kept at these conditions under stirring for 40 minutes. The reaction was terminated by quickly removing the reactor from the furnace and immersing it into an ice bath.

The hydrogenation of limonene was performed in $scCO_2$ in a batch reactor. A given amount of Ru-catalyst (20-50 mg, depending on the catalyst), 1 mL of limonene and a stirring bar were placed in the 60 mL high-pressure reactor. The reactor was sealed and purged with H_2 at low pressure several times. Then, the reactor was heated at 50ºC and 16.0 MPa of CO_2 were added from a thermostated ISCO syringe pump (Isco, Inc. Model 260D). Reaction was started by adding 4.0 MPa of H_2 to the reactor. Reaction was kept at these conditions under stirring for 15-60 minutes. The reaction was terminated by quickly removing the reactor from the furnace and immersing it into an ice bath.

Reaction mixture was recovered by washing the reactor with small amounts of dichloromethane or hexane for the benzene and limonene hydrogenation reactions, respectively. The solid catalyst was separated from the reaction mixture by filtration and when necessary, organics were recovered by liquid extraction using a separating funnel. Reaction products were analysed by a GC-2010 Plus Shimadzu gas chromatograph equipped with a flame ionization detector (FID). A Zebron ZB-1HT capillary column (20 m x 0.18 mm i.d. x 0.18 μm film thickness) was used for the separation. N_2 was used as carrier gas. For the hydrogenation of benzene, oven temperature was programmed at 35 ºC for 10 minutes. Injector and detector temperature was 280 ºC with a split ratio of 150. Identification of the products was performed by comparison with high-purity standards. In the hydrogenation of limonene, the oven temperature was programmed from 87-91 ºC ramp at 0.5 ºC/min, and 91-240 ºC ramp at 20ºC/min. Injector and detector

temperature was 250 ºC with a split ratio of 300. A GC/MS CP-3800 coupled to a MS Varian model Saturno 2200 Ion Trap equipped with a Zebron ZB-5MS capillary column (30 m x 0.25 mm i.d. x 0.25 μm film thickness) was used for the product identification. He gas was used as carrier at 1 mL/min. Oven temperature was programmed at 55 ºC for 2 minutes, then from 55-80 ºC ramp at 3 ºC/min and 80-290 ºC ramp at 2 0ºC/min.

3. Results and discussion

Ru was deposited on mesoporous SiO_2 SBA-15 using $scCO_2$ following the different procedures previously outlined. The materials were then tested in hydrogenation reactions. A summary of the experiments conducted is given in Table 1.

3.1. Ru deposition experiments by impregnation

Deposition experiments by the impregnation method were performed using $Ru(tmhd)_2(COD)$ on SiO_2 at 80 ºC and 13.5 and 19.3 MPa. The amount of precursor adsorbed on the support was determined by TGA analysis of the impregnated samples in N_2 flow and values close to 30 and 13 mass % were obtained for samples 1 and 2 obtained at 13.5 and 19.3 MPa, respectively at the same $Ru:SiO_2$ molar ratio (see Supplementary material). Considering that the total weight loss is due to the precursor ligands, the amount of $Ru(tmhd)_2(COD)$ remaining in CO_2 after adsorption at these conditions is below its solubility limit.[49] The amount adsorbed decreased as the pressure and density of the supercritical phase increased, in agreement with previous reports.[15] At high pressure, both the solubility of the precursor in the fluid phase and the concentration of CO_2 increased and consequently, the partition coefficient of the precursor changed, lowering its adsorption on the surface.

After impregnation, samples were reduced in N_2/H_2 at 400 ºC. XRD analysis of samples 1 and 2 obtained by impregnation at 80ºC and 13.5 and 19.3 MPa and further reduction are shown in Figure 1. Wide angle XRD reveals the presence of a very broad and intense reflection at 2θ *ca.* 22 which is due to the amorphous SiO_2 support, as well as minor peaks at ca. 42 and 44 º assigned to the (002) and (101) reflexions of hexagonal Ru (PDF 06-0663). Ru peaks are very broad suggesting that particles are very small. The intensity of the Ru peaks is much lower for sample 2 impregnated at the higher pressure.

TEM images of the Ru/SiO_2 samples 1 and 2 obtained by impregnation in $scCO_2$ at 80ºC and further reduction in H_2/N_2 are shown in Figure 2. Mesoporous silica SBA-15 is a highly porous support formed by an hexagonal array of one-dimensional cylindrical mesopores interconnected through smaller micro and mesopores.[53, 54] The mesoporous channels of the SiO_2 SBA-15 structure along with small darker Ru nanoparticles may be observed in Figure 2. Particles are very small, more or less spherical and homogeneously dispersed. Similar results have been previously obtained for the deposition of Pd nanoparticles on mesoporous SiO_2.[15, 55] The particle diameter is well below the pore size of the support, particularly for sample 2 impregnated at the higher pressure. TEM images clearly show that the number and size of the Ru nanoparticles are much larger when the impregnation is performed at the lower pressure in agreement with previous results. At the 1:19 $Ru:SiO_2$ molar ratio, the Ru content determined by EDX analysis varied from 0.9 to 1.5% mol for the samples prepared at 80 ºC and 13.5 and 19.3 MPa, respectively (average of several images).

For selected samples the Ru content was also determined by XRF as previously described. For a sample containing a 0.9% Ru mol determined by EDX, 1.2% Ru mol

was measured by XRF. Considering the good agreement among the different techniques and the errors associated to each of them, for comparison purposes, the % Ru determined by EDX was used to quantify the Ru content in the samples as shown in Table 1.

The expected Ru mol percentage considering the precursor uptake measured by TGA (see supplementary material†) was higher than the Ru mol percentage measured in the samples reduced by the different techniques, which indicated the partial loss of the precursor during the thermal reduction. TGA analysis of the precursor $Ru(tmhd)_2(COD)$ showed that this compound sublimes between 200-275 ºC in N_2. However, TGA analysis of a SiO_2 support impregnated with $Ru(tmhd)_2(COD)$ revealed different weight loss events, the first one related to the sublimation of the precursor adsorbed on SiO_2 at temperatures below 250 ºC. ºC. At higher temperatures, the weight loss is associated to the decomposition of the precursor to its metal form. In contrast, when $Ru(tmhd)_2(COD)$ was adsorbed on CA in $scCO_2$, the sublimation of the precursor did not take place in N_2 atmosphere.[23] These results indicate that the hydrophilic SiO_2 support interacts weakly with the precursor.

3.2. Ru deposition experiments by reactive deposition with H_2

H_2-reduction of $Ru(tmhd)_2(COD)$ on SiO_2 SBA-15 was also performed. The precursor dissolution was carried out at 80 ºC and 13.5 MPa and the reduction was performed at 150 ºC in the H_2/CO_2 mixture. XRD analysis of a Ru/SiO_2 SBA-15 sample obtained following this procedure (sample 3) is shown in Figure 3, showing strong reflections due to Ru (PDF 06-0663). The intensity of the peaks is much higher than that observed in the samples obtained by impregnation. Nevertheless, the peaks are very broad, which suggests that particles are very small.

TEM images of sample 3 obtained by H_2-reduction of $Ru(tmhd)_2(COD)$ are shown in Figure 4. As in previous examples, small dark Ru nanoparticles are deposited into the mesopores of the support. The size of the particles is constrained by the pore size of the support. The average Ru content by EDX on this sample was ca. 6.0% mol Ru. Comparison with images shown in Figures 2a-b for materials obtained by impregnation in $scCO_2$ at 80ºC and 135 bar and reduction in H_2/N_2 revealed that particles in Figure 4 have grown slightly and turned into small rods. The deposition of Ru is a self-catalytic process and once it is started, the small Ru nanoparticles act as catalytic centres for the precursor reduction. Nevertheless, this material remained very homogeneous. Considering the amounts of $Ru(tmhd)_2(COD)$ and substrate loaded into the reactor, the precursor decomposition in H_2/CO_2 is complete.

3.3. Ru deposition experiments by reactive deposition with EtOH

The deposition of Ru on SiO_2 SBA-15 was also attempted in CO_2/EtOH mixtures with EtOH as the reducing agent. Experiments were performed using $Ru(tmhd)_2(COD)$ and $RuCl_3 \cdot xH_2O$ as precursors. Dissolution was carried out at 80 ºC and 13.5 MPa for $Ru(tmhd)_2(COD)$ and at 35 ºC and 8.5 MPa for $RuCl_3 \cdot xH_2O$ in the EtOH/CO_2 mixture. In both cases the reduction was initiated by heating the reaction mixture. Experiments performed using $Ru(tmhd)_2(COD)$ showed the incomplete decomposition of the precursor even at 200 ºC, which could be assessed by the weak colour change of the SiO_2 support from white to slightly grey and the dark brown colour of the solution obtained after venting the supercritical phase through acetone (not shown in Table 1). On the contrary, Ru was successfully deposited on the support from $RuCl_3 \cdot xH_2O$ at 150-200 ºC in the supercritical mixture (10% mol EtOH in CO_2) yielding dark grey/black products (samples 4-6).

XRD patterns of the different Ru/SiO_2 samples obtained following this procedure are shown in Figure 5. XRD of the samples shown in Figures 5a and b were obtained using similar or lower $RuCl_3 \cdot xH_2O$ to support molar ratios than in previous experiments (1:28 and 1:48) and at the decomposition temperature of 150 and 200 ºC, samples 4 and 5 respectively. However, XRD of sample 6 shown in Figure 5c corresponds to a material obtained at the lower temperature using a much higher precursor to support ratio (1:6). Apart from the wide reflection of the support, XRD of the sample obtained with the higher precursor to support molar ratio (sample 6) showed the presence of very broad bands at 2θ values *ca.* 38.4, 42.2 and 44.0 due to Ru (PDF 06-0663). In contrast, the samples produced at the lower ratios at both temperatures (samples 4 and 5) did not show clearly the presence of Ru in the XRD pattern, which may be related to the low metal concentration and the small metal particle size.

Figure 6 shows TEM images of the samples obtained by the alcohol assisted reduction of $RuCl_3 \cdot xH_2O$ at 150 and 200 ºC. In every case, mesopores in the support were filled with Ru metal nanoparticles whose size was limited by the pore size of the support. The amount of Ru determined by EDX in the different samples varied as a function of deposition temperature and concentration. The amount of Ru deposited at 150 ºC increased as the $Ru:SiO_2$ molar ratio increased, and values of 0.8% and 7.4% mol Ru were measured by EDX for sample 4 (Figures 6a-b) and sample 6 (Figures 6 e-f), respectively. These values were lower than those expected taking into account the amounts of $RuCl_3 \cdot xH_2O$ and support loaded into the reactor; 2.0 and 10.0% Ru mol for samples 4 and 5, respectively. The lower Ru loads obtained at 150 ºC indicated the incomplete precursor decomposition. For sample 5 deposited at 200 ºC, the percentage Ru mol determined by EDX was equal to 3.2%. This value is very similar to the

maximum expected (3.4% mol). Increasing the deposition temperature at 200 ºC favours the incorporation of the metal into the support.

Ru nanoparticles for the samples deposited at 150 ºC and the different concentrations were homogeneously distributed throughout the support. In contrast, in sample 5 obtained at 200 ºC, Ru nanoparticles arranged together forming long nanowires. Ru nanoparticles deposited acted as catalytic sites for the precursor reduction and less homogeneous materials were obtained at 200 ºC. At 150 ºC this effect was not so important and uniformly distributed particles were obtained at the different compositions studied.

EDX analysis revealed the presence of chlorine impurities in the different samples deposited using EtOH, which may be due to the unreacted precursor or to reaction by-products impurities.

3.4. N_2 adsorption-desorption isotherms

The porosity of the Ru/SiO_2 SBA-15 composite materials was further studied by N_2-adsorption. Table 1 shows S_{BET}, pore volume (V_p) and pore size obtained from the adsorption isotherms for the SiO_2 and Ru/SiO_2 samples. Figure 7 compares the adsorption isotherms and pore size distributions of the Ru/SiO_2 samples prepared by impregnation at 80 ºC and 13.5 MPa (sample 1), and H_2 reduction at 150 ºC (sample 3). Data for the rest of the samples presented in Table 1 are given as Supplementary material.† Isotherms exhibit a type IV, subtype H1, hysteresis loop which is found in mesoporous materials with well-defined cylindrical-like pore channels. BET surface area of the support was 571 m^2/g and pore volume was 0.80 cm^3/g. Adsorption isotherms for the samples produced by impregnation at 13.5 and 19.3 MPa (samples 1

and 2) were very similar to those of the support (for clarity not shown here), particularly in the adsorption branch of the isotherms. The desorption branch of the isotherm however changed, as it will be explained later, due to the presence of Ru nanoparticles into the mesopores. Due to the small amount of Ru deposited and the small particle size, deposition of Ru by impregnation into the support (samples 1 to 2) led to S_{BET} and Vp values very similar to those of the SiO_2 sample. However, S_{BET} measured for sample 3 obtained by H_2-reduction was reduced to 438 m^2/g and the pore volume to 0.66 cm^3/g most likely due to the much larger Ru content. Analysis of the pore size distribution of the SiO_2 SBA-15 support obtained from the adsorption branch of the isotherm gave a narrow pore size distribution with a maximum at 6.8 nm. In comparison, there was only a slight reduction of the pore size in all the Ru/SiO_2 samples.

Similar results were found for samples 4 to 6 reduced using EtOH (see Table 1 and supplementary material). For sample 6, with the highest Ru content, S_{BET} was reduced to 435 m^2/g and the pore size decreased from ca. 7.0 to 6.4 nm. For samples 5 and 6, S_{BET} was reduced in a similar way. Comparison of samples 2 and 4, containing very similar Ru mol percentages but prepared by different techniques, showed much lower S_{BET} and Vp values in sample 4 deposited using EtOH. This sample showed the highest reduction in the pore volume. This could be related to the presence of unreacted $RuCl_3 \cdot xH_2O$ or reaction by-products in the samples deposited using EtOH that were already detected by EDX and suggests the need to incorporate a washing step when the reaction is performed by reactive deposition with EtOH.

The pore size distributions estimated from the desorption branch of the isotherm of all the Ru/SiO_2 composite materials showed a new maximum at ca. 3.6 nm. This phenomenon is often referred as tensile strength effect and it is due to ink-bottle like

sections created by the nanoparticles in the mesopores. Similar adsorption-desorption isotherms have been previously reported for partially plugged hexagonal templated silica (PHTS). [54] The maximum at 3.6 nm depends on the adsorptive used (in our case N_2). These data indicate that the presence of Ru narrows at least part of the mesopores in SBA-15 in all the samples. However, the fact that the pore volume remains high in the Ru/SiO_2 samples indicates that the pores are still accessible to the gas molecules after deposition. The interconnected mesopores in SiO_2-SBA-15 may facilitate this process.

3.5 Catalytic tests

The catalytic performance of some of the Ru/SiO_2 SBA-15 samples synthesized using supercritical CO_2 was assessed for the hydrogenation reactions of benzene and limonene (schemes 2 and 3, respectively). Tables 2 and 3 summarise the results obtained. The catalytic activity was compared to that of a 5% mass Ru on carbon commercial catalyst purchased from Strem Chemical.

Total conversion *(*%C), selectivity *(*%S_i) and yield (%Y_i) of product i were defined as:

$$C(\%) = \frac{\sum C_P}{\sum C_P + C_R^{un}} \times 100\% \qquad S_i(\%) = \frac{C_i}{\sum C_P} \times 100\% \qquad Y_i(\%) = \frac{C_i}{\sum C_P + C_R^{un}} \times 100\%$$

where C_i *is* the concentration of the intermediate product (cyclohexene or *p*-menthene), $\sum C_P$ is the total concentration of the hydrogenation products and C_R^{un} is the concentration of the unreacted reactant. Quantification was performed by integrated peak area normalization.

The Turnover Frequency (TOF) was estimated considering the Ru content measured by EDX as follows

$$TOF = \frac{mole\ reactant \times C(\%)}{mol\ Ru \times time(h)}$$

Table 2 summarizes the benzene hydrogenation catalytic tests. Cyclohexene and cyclohexane were identified by GC-FID as the only reaction products, by comparison of the retention times with external standards. Experiments were performed without solvent at 40 ºC and in a $ZnSO_4$ aqueous solution at 150 ºC for 15 and 40 minutes. The reaction without solvent proceeded at 40 ºC to completion to the fully hydrogenated product cyclohexane in 40 minutes when the commercial Ru/C catalyst was used. Comparatively, the Ru/SiO_2 catalyst prepared by reactive deposition in H_2/CO_2 (sample 3) gave a lower conversion without much selectivity to cyclohexene. Diffusion of reactants to the inner surface of the mesoporous catalyst may be hindered in the liquid phase at such a low temperature. On the other hand, when the reaction was carried out in the $ZnSO_4$ aqueous solution at 150 ºC using the same Ru/SiO_2 catalyst, although the conversion was low, total selectivity to cyclohexene was obtained. The conversion was higher when the Ru/C catalyst was used, but the process was not selective to cyclohexene. Furthermore, the benzene to Ru molar ratio was lower and as a result the TOF was lower. However, cyclohexene yield using the Ru/SiO_2 SBA-15 catalyst prepared in this study was lower than those obtained using other Ru/SiO_2 catalysts at similar conditions.[56] The partial degradation of the SiO_2 SBA-15 support at the reaction conditions in the aqueous medium may cause the lower conversion.[57] Due to the limitations of the support for this reaction, no further optimization of the process was performed.

The Ru/SiO_2 materials obtained by the alcohol reduction in $scCO_2$ were also tested in the benzene hydrogenation. Conversion in this case was very low even for the catalysts

with a very high Ru content, which could be related to the presence of chlorine impurities in these samples (determined by EDX). Further washing of the samples in this case would be required.

To avoid the use of water and to improve the mass transport, the hydrogenation of limonene in $scCO_2$ was chosen as a model reaction. Table 3 summarises the results. Reactions were performed for 15, 30 and 60 min employing the Ru/SiO_2 catalysts produced by H_2-reaction (sample 3) and impregnation (sample 1) and were compared to the same reaction using the commercial Ru/C catalyst. Reaction products are the intermediate product *p*-menthene (*p*-menth-1-ene and *p*-menth-3-ene) and the fully hydrogenated compounds *cis*-*p*-mentane and *trans*-*p*-menthane in a 4:5 ratio in agreement with previous reports.[46] Complete conversion was achieved with every catalyst at 60 and 30 min. At these reaction times, selectivity to *p*-menthene was very low for the Ru/C catalyst but it was higher for the Ru/SiO_2 catalyst obtained by H_2-reduction. After 30 min, this catalyst gave a yield to *p*-menthene equal to 63%. On the other hand, the catalyst obtained by impregnation in $scCO_2$ (sample 1) rendered a conversion equal to 100% after 15 minutes but no selectivity to *p*-menthene.

For the commercial Ru/C and the Ru/SiO_2 catalyst obtained by H_2-reduction (sample 3), the conversion decreased to 90% at 15 min, but the selectivity increased. The highest selectivity was obtained for the Ru/SiO_2 catalyst obtained by H_2-reduction with a value close to 80%, which represents a yield to *p*-menthene of 69%. This reaction yield is larger than those obtained by Nunes da Ponte and co-workers at very similar conditions using other Pd/C and Pt/C catalysts[44, 45, 58, 59] and slightly lower than those obtained by the same group for Ru/Al_2O_3 coated with screened imidazolium ionic liquids catalysts using larger Ru to limonene ratios.[46]

The results suggest a correlation between conversion, selectivity and Ru particle size. The particle size in the catalyst obtained by impregnation in $scCO_2$ (sample 1) is very small and the metal dispersion is very good, and as a result the conversion to the fully hydrogenated product is very high after 15 minutes. On the other hand, the catalyst obtained by H_2-reduction (sample 3) is not so active but more selective to the intermediate product. Ru nanoparticles in this case are larger and slightly elongated. Other authors have suggested a similar relationship between selectivity and particle size for other selective hydrogenation reactions. [60] Further experiments should be conducted in order to confirm these findings.

4. Conclusions

The deposition of Ru nanoparticles on a mesoporous SiO_2 SBA-15 support has been successfully carried out using $Ru(COD)(tmhd)_2$ and $RuCl_3 \cdot xH_2O$ in $scCO_2$. Three different reaction routes have been tried: impregnation in $scCO_2$ and reduction in H_2/N_2 at low pressure, reactive deposition with H_2 in $scCO_2$, and reactive deposition with ethanol in $scCO_2$. In every case, Ru nanoparticles were deposited within the mesopores of the SiO_2 SBA-15. When $scCO_2$ was used only as impregnation medium, Ru load was controlled by the adsorption equilibrium of the precursor on the support and, at 80 ºC samples with 1.5 and 0.9% mol Ru were obtained at 13.5 and 19.3 MPa, respectively. Particles were very small and appeared very homogeneously distributed throughout the mesoporous support. Furthermore, due to the small particle size, there was almost no reduction of the BET surface area. Similar Ru/SiO_2 SBA-15 materials were obtained by the reactive deposition with H_2 at 150 ºC. In this case, however, a much larger Ru load was obtained (6.0% mol) for the same initial metal concentrations and the reaction proceeded to completion. Particles in this case were slightly larger and aggregated into

small rods. On the other hand, the reactive deposition of $RuCl_3 \cdot xH_2O$ in $EtOH/CO_2$ was successful at very mild conditions (150-200 ºC). This is a very promising result because metal chlorides are cheaper precursors, less toxic and easier to handle than organometallic compounds. In this case, EtOH was the cosolvent that allowed the dissolution of the $RuCl_3 \cdot xH_2O$ salt in $scCO_2$ and, at the same time, the reducing agent that yielded Ru nanoparticles. Although the precursor decomposition was complete only at 200 ºC, loads between 0.8 and 7.4% mol Ru were obtained by varying the precursor concentration and temperature. Ru nanoparticles were homogeneously distributed throughout the support particularly at 150 ºC. At 200 ºC and low precursor to support molar ratio, particles appeared connected within the mesopores forming nanowires. Further washing of the samples is required.

The Ru/SiO_2 SBA-15 composite materials prepared in $scCO_2$ were tested as heterogeneous catalysts in the partial hydrogenation reactions of benzene and limonene. In the hydrogenation of benzene in a $ZnSO_4$ aqueous solution at 150 ºC, the catalyst prepared by H_2-reduction in $scCO_2$ was more selective to the intermediate product cyclohexene than a commercial Ru/C catalyst. Similarly, in the hydrogenation of limonene in $scCO_2$ at 50ºC, the same catalyst gave the best yields to the intermediate product *p*-menthene, with values close to 70% in 15 minutes. These values are comparable or better than others previously reported in the literature. On the other hand, the Ru/SiO_2 catalyst prepared by impregnation gave the highest conversion at 15 min but no selectivity to *p*-menthene, probably due to the smaller particle size.

Supercritical CO_2 is a green solvent that allows the preparation of efficient selective heterogeneous catalysts and that it can be also used as the solvent to perform the hydrogenation reaction.

ACKNOWLEDGEMENTS

We gratefully acknowledge the financial support of the Spanish Ministry of Economy and Competitiveness (MINECO), research projects CTQ2013-41781-P and MAT2013-44964-R. J. Morère thanks MINECO for his support through a predoctoral grant. We thank Dr. Y. Sánchez-Vicente and Dr. N. Kayali for helpful discussion. We also thank "ICTS- Centro Nacional de Microscopía Electrónica", "Centro de Rayos X" and "Centro de Espectrometría de Masas" at UCM for technical assistance.

NOTES AND REFERENCES

[a] Department of Physical Chemistry I, Universidad Complutense de Madrid, 28040 Madrid. SPAIN

[b] Department of Inorganic Chemistry I, Universidad Complutense de Madrid, 28040 Madrid. SPAIN

† Electronic Supplementary Information (ESI) available: TGA of the precursor $Ru(tmhd)_2(COD)$ and the impregnated samples. N_2-adsorption desorption isotherms and pore size distributions of some samples.

‡ CAUTION: These experiments involve high-pressure and/or temperature and they should be only performed with caution using appropriate high-pressure equipment and safety precautions.

1. P. Kluson and L. Cerveny, *Appl. Catal. A-Gen.*, 1995, **128**, 13-31.
2. P. Kluson and L. Cerveny, *J. Mol. Cata. A: Chem.*, 1996, **108**, 107-112.
3. P. Kluson, J. Had, Z. Belohlav and L. Cerveny, *Appl. Catal. A-Gen.*, 1997, **149**, 331-339.
4. H. Liu, T. Jiang, B. X. Han, S. Liang, W. Wang, T. Wu and G. Y. Yang, *Green Chemistry*, 2011, **13**, 1106-1109.
5. P. Gallezot, *Catal. Today*, 2007, **121**, 76–91.
6. P. Kluson, L. Cerveny and J. Had, *Catal. Lett.*, 1994, **23**, 299-312.

7. A. I. Carrillo, L. C. Schmidt, M. L. Marin and J. C. Scaiano, *Catal. Sci. Technol.*, 2014, **4**, 435-440.
8. J. Alvarez-Rodriguez, I. Rodriguez-Ramos, A. Guerrero-Ruiz, E. Gallegos-Suarez and A. Arcoya, *Chem. Eng. J.*, 2012, **204**, 169-178.
9. T. Wu, P. Zhang, J. Ma, H. Fan, W. Wang, T. Jiang and B. X. Han, *Chinese J. Catal.*, 2013, **34**, 167-175.
10. S. D. Miao, Z. Liu, B. X. Han, J. Huang, Z. Y. Sun, J. L. Zhang and T. Jiang, *Angew. Chem. Inter. Ed.*, 2006, **45**, 266-269.
11. R. J. White, R. Luque, V. L. Budarin, J. H. Clark and D. J. Macquarrie, *Chem. Soc. Rev.*, 2009, **38**, 481-494.
12. Y. Zhang and C. Erkey, *J. Supercrit. Fluids*, 2006, **38**, 252-267.
13. C. Erkey, *J. Supercrit. Fluids*, 2009, **47**, 517-522.
14. X. Zang, S. Heinonen and L. E., *RSC Adv.*, 2014, **4**, 61137-61152.
15. M. J. Tenorio, C. Pando, J. A. R. Renuncio, J. G. Stevens, R. A. Bourne, M. Poliakoff and A. Cabanas, *J. Supercrit. Fluids*, 2012, **69**, 21-28.
16. Y. Sánchez-Vicente, S. L., C. Pando, M. J. Torralvo, C. E. Snape, T. C. Drage and A. Cabañas, *Chem. Eng. J.*, 2015, **264** 886–898.
17. D. L. Tomasko, H. B. Li, D. H. Liu, X. M. Han, M. J. Wingert, L. J. Lee and K. W. Koelling, *Ind. Eng. Chem. Res.*, 2003, **42**, 6431-6456.
18. K. S. Morley, P. C. Marr, P. W. Webb, A. R. Berry, F. J. Allison, G. Moldovan, P. D. Brown and S. M. Howdle, *J. Mater. Chem.*, 2002, **12**, 1898-1905.
19. J. J. Watkins and T. J. McCarthy, *Chem. Mater.*, 1995, **7**, 1991-&.
20. J. J. Watkins, J. M. Blackburn and T. J. McCarthy, *Chem. Mater.*, 1999, **11**, 213-215.
21. E. Kondoh, *Jpn. J. Appl. Phys. 1*, 2005, **44**, 5799-5802.
22. A. O´Neil and J. Watkins, *Chem. Mater.*, 2006, **18**, 5652-5658.
23. Y. Zhang, D. Kang, M. Aindow and C. Erkey, *J. Phys. Chem.B*, 2005, **109**, 2617-2624.
24. Y. Lin, X. Cui, C. H. Yen and C. M. Wai, *Langmuir*, 2005, **21**, 11474-11479.
25. C. F. Karanikas and J. Watkins, *Microelectron. Eng.*, 2010, **87**, 566-572.
26. E. Kondoh, *Jpn. J. Appl. Phys. 1*, 2004, **43**, 3928-3933.
27. X.-R. Ye, Y. Lin, C. Wang, M. H. Engelhard, Y. Wang and C. M. Wai, *J. Mater. Chem.*, 2004, **14**, 908-913.
28. Z. Sun, Z. Liu, B. Han, S. Miao, Z. Miao and G. An, *J. Colloid Interface. Sci.*, 2006, **304**, 323-328.
29. Y. J. Zhao, J. L. Zhang, J. L. Song, J. S. Li, J. L. L, T. B. Wu, P. Zhang and B. X. Han, *Green Chemistry*, 2011, **13**, 2078-2082.
30. Z. Y. Sun, L. Fu, Z. M. Liu, B. X. Han, Y. Q. Liu and J. M. Du, *J. Nanosci. Nanotechnol.*, 2006, **6**, 691-697.

31. Z. Y. Sun, Z. M. Liu, B. X. Han, Y. Wang, J. M. Du, Z. L. Xie and G. J. Han, *Adv. Mater.*, 2005, **17**, 928-932.
32. J. Zhao, W. B. Hu, H. Q. L., M. Ji, C. Z. Zhao, Z. B. Wang and H. Q. Hu, *RSC Adv.*, 2015, **5**, 7679-7686.
33. C. V. Yen, H. W. Lin, T. D. Phan and C.-S. Tan, *J. Nanosc. Nanotech.*, 2011, **11**, 2465-2469.
34. Y. Zhang, B. Cangul, Y. Garrabos and C. Erkey, *J. Supercrit. Fluids*, 2008, **44**, 71-77.
35. M. Ge, F. Ding and C. Erkey, *Adv. Mater. Res.*, 2012, **418-420**, 2260-2264.
36. G. Caputo, I. De Marco and E. Reverchon, *J. Supercrit. Fluids*, 2010, **54**, 243-249.
37. H. Wakayama and Y. Fukushima, *J. Chem. Eng. Japan*, 2009, **42**, 134-138.
38. Y. Zhang, H. Jiang, Y. Wang and M. Zhang, *Ind. Eng. Chem. Res.*, 2014, **53**, 6380-6387.
39. S. K. Xu, P. Zhang, H. B. Li, H. J. Wei, L. M. Li, B. J. Li and W. X.Y., *RSC Adv.*, 2014, **4**, 7079-7083.
40. E. J. Beckman, *J. Supercrit. Fluids*, 2004, **28**, 121–191.
41. W. Leitner, *Acc. Chem. Res.* , 2002, **35**, 746-756.
42. P. Licence, K. Ke, M. Sokolova, S. K. Ross and M. Poliakoff, *Green Chemistry*, 2003, **5**, 99-104.
43. C. Y. Tsang and W. B. Street, *Chem. Eng. Sci.*, 1981, **36**, 993-1000.
44. E. Bogel-Lukasik, I. Fonseca, R. Bogel-Lukasik, Y. A. Tarasenko, M. N. da Ponte, A. Paiva and G. Brunner, *Green Chemistry*, 2007, **9**, 427-430.
45. E. Bogel-Lukasik, R. Bogel-Lukasik and M. N. da Ponte, *Monatsh. Chem.*, 2009, **140**, 1361-1369.
46. E. Bogel-Lukasik, S. Santos, R. Bogel-Lukasik and M. N. da Ponte, *J. Supercrit. Fluids*, 2010, **54**, 210-217.
47. D. Y. Zhao, Q. S. Huo, J. L. Feng, B. F. Chmelka and G. D. Stucky, *J. Am. Chem. Soc.*, 1998, **120**, 6024-6036.
48. D. Y. Zhao, J. L. Feng, Q. S. Huo, N. Melosh, G. H. Fredrickson, B. F. Chmelka and G. D. Stucky, *Science*, 1998, **279**, 548-552.
49. J. Morere, M. Jose Tenorio, C. Pando, J. A. R. Renuncio and A. Cabanas, *J. Chem. Thermodyn.*, 2013, **58**, 55-61.
50. M. Jaroniec, M. Kruk and J. P. Olivier, *Langmuir*, 1999, **15**, 5410-5413.
51. E. Barret, L. G. Joyner and P. P. Halenda, *J. Am. Chem. Soc.*, 1951, **73**, 373-380.
52. E. V. Spinace and J. M. Vaz, *Catal. Commun.*, 2003, **4**, 91-96.
53. M. Kurk, M. Janoriec, C. H. ko and R. Ryoo, *Chem. Mater.*, 2000, **12**, 1961-1968.
54. V. Meynen, P. Cool and E. F. Vansant, *Micropor. Mesopor. Mater.*, 2007, **104**, 26-38.

55. J. Morere, M. J. Tenorio, M. J. Torralvo, C. Pando, J. A. R. Renuncio and A. Cabanas, *J. Supercrit. Fluids*, 2011, **56**, 213-222.

56. J. Ning, J. Xu, J. Liu and F. Lu, *Catal. Lett.*, 2006, **109**, 175-780.

57. A. Galarneau, M. Nader, F. Guenneau, F. Di Renzo and A. Gedeon, *J. Phys. Chem. C.*, 2007, **111**, 8268-8277.

58. E. Bogel-Lukasik, R. Bogel-Lukasik and M. N. da Ponte, *Ind. Eng. Chem. Res.*, 2009, **48**, 7060-7064.

59. E. Bogel-Lukasik, R. Bogel-Lukasik, K. Kriaa, I. Fonseca, Y. Tarasenko and M. Nunes da Ponte, *J. Supercrit. Fluids*, 2008, **45**, 225-230.

60. A. K. Prashar, S. Mayadevi and R. Nandini Devi, *Catal. Commun.*, 2012, **28**, 42-46.

Table 1. Summary of Ru deposition experiments on SiO_2 SBA-15 using $scCO_2$.

Sample	Methodology $scCO_2$	Precursor	$Ru:SiO_2$[a]	% Ru mol (EDX)	SiO_2			Ru/SiO_2		
					S_{BET} (m^2/g)	Pore size (nm)	Vp (cm^3/g)	S_{BET} (m^2/g)	Pore size (nm)	Vp (cm^3/g)
1	Impregnation 80ºC 13.5 MPa	$Ru(tmhd)_2(COD)$	1:19	1.5	571	6.8	0.80	571	6.6	0.78
2	Impregnation 80ºC 19.3 MPa	$Ru(tmhd)_2(COD)$	1:19	0.9	571	6.8	0.80	544	6.4	0.73
3	H_2 reactive deposition 150 ºC	$Ru(tmhd)_2(COD)$	1:20	6.0	581	6.7	0.81	438	6.5	0.66
4	EtOH reactive deposition 150 ºC	$RuCl_3 \cdot xH_2O$	1:48	0.8	571	6.8	0.80	447	6.1	0.47
5	EtOH reactive deposition 200 ºC	$RuCl_3 \cdot xH_2O$	1:28	3.2	571	6.8	0.80	470	6.2	0.67
6	EtOH reactive deposition 150 ºC	$RuCl_3 \cdot xH_2O$	1:6	7.4	564	7.0	0.78	435	6.4	0.69

[a] Initial $Ru:SiO_2$ molar ratio

Table 2. Summary of the benzene hydrogenation experiments using different Ru catalysts.

Method	Sample	Methodology $scCO_2$	% Ru EDX[a]	Time (min)	*C*(%)	*S*(%)[b]	*Y*(%)[b]	Benzene :Ru[c]	TOF x 10^{-3} (h^{-1})
(1) No solvent	3	H_2 reactive deposition 150 ºC	9.7	15	<1	0	0	860	-
				40	64	2	1	800	76
	Strem	Ru/C	5.0	15	7	0	0	1040	27
				40	100	0	0	1120	170
(2) $ZnSO_4$ (aq.)	3	H_2 reactive deposition 150 ºC	9.7	40	17	100	17	890	23
	Strem	Ru/C	5.0	40	30	0	0	500	22

[a] percentage by mass; [b] *S* and *Y* for cyclohexene; [c] molar ratio

Table 3. Summary of the limonene hydrogenation experiments using different Ru catalysts.

Sample	Methodology $scCO_2$	% Ru EDX[a]	Time (min)	*C*(%)	*S*(%)[b]	*Y*(%)[b]	Limonene :Ru[c]	TOF x 10^{-3} (h^{-1})
3	H_2 reactive deposition 150 ºC	9.7	60	100	4	4	480	48
			30	100	63	63	560	110
			15	90	77	69	660	240
1	Impregnation 80ºC and 13.5 MPa	2.5	15	100	0	0	550	220
Strem	Ru/C	5.0	60	100	6	6	420	42
			30	100	41	41	540	110
			15	93	62	58	540	200

[a] percentage by mass; [b]*S* and *Y* for *p*-menthene; [c] molar ratio

Figure captions

Scheme 1. Summary of the Ru deposition experiments performed by impregnation and reactive deposition using H_2 and EtOH.

Scheme 2. Reaction pathway for the hydrogenation of benzene.

Scheme 3. Main reaction pathway for the hydrogenation of limonene [58].

Figure 1. XRD of the Ru/SiO_2 SBA-15 samples obtained by impregnation of $Ru(tmhd)_2(COD)$ in $scCO_2$ at 80ºC and: (a) 13.5 MPa (sample 1) and (b) 19.3 MPa (sample 2), after reduction in H_2/N_2.

Figure 2. TEM images of Ru/SiO_2 SBA-15 samples obtained by impregnation of $Ru(tmhd)_2(COD)$ in $scCO_2$ at 80ºC and: (a,b) 13.5 MPa (sample 1) and (c, d) 19.3 MPa (sample 2), after reduction in H_2/N_2.

Figure 3. XRD pattern of a Ru/SiO_2 SBA-15 sample obtained by the H_2-reduction of $Ru(tmhd)_2(COD)$ in $scCO_2$ at 150 ºC (sample 3).

Figure 4. TEM images of a Ru/SiO_2 SBA-15 sample obtained by the H_2-reduction of $Ru(tmhd)_2(COD)$ in $scCO_2$ at 150 ºC (sample 3).

Figure 5. XRD pattern of the Ru/SiO_2 SBA-15 samples obtained by the alcohol reduction of $RuCl_3 \cdot xH_2O$ in $scCO_2$ at different temperatures and/or precursor to support molar ratios: (a) 150 ºC and 1:48 $Ru:SiO_2$ molar ratio (sample 4), (b) 200 ºC and 1:28 $Ru:SiO_2$ molar ratio (sample 5), (c) 150 ºC and 1:6 $Ru:SiO_2$ molar ratio (sample 6).

Figure 6. TEM images of the Ru/SiO_2 SBA-15 samples obtained by the alcohol reduction of $RuCl_3 \cdot xH_2O$ in $scCO_2$ at different temperatures and/or precursor to support

molar ratios: (a) 150 ºC and 1:48 Ru:SiO_2 molar ratio (sample 4), (b) 200 ºC and 1:28 Ru :SiO_2 molar ratio (sample 5), (c) 150 ºC and 1:6 Ru :SiO_2 molar ratio (sample 6).

Figure 7. N_2 Adsorption-desorption isotherms (a) and pore size distributions obtained from the adsorption (b) and desorption (c) branches of the isotherm for: (○) Ru/SiO_2 SBA-15 obtained by impregnation of $Ru(tmhd)_2(COD)$ in $scCO_2$ at 80ºC and 13.5 MPa and further reduction in H_2/N_2 (sample 1) and (□) Ru/SiO_2 SBA-15 obtained by H_2-reduction of $Ru(tmhd)_2(COD)$ in $scCO_2$ at 150 ºC (sample 3).

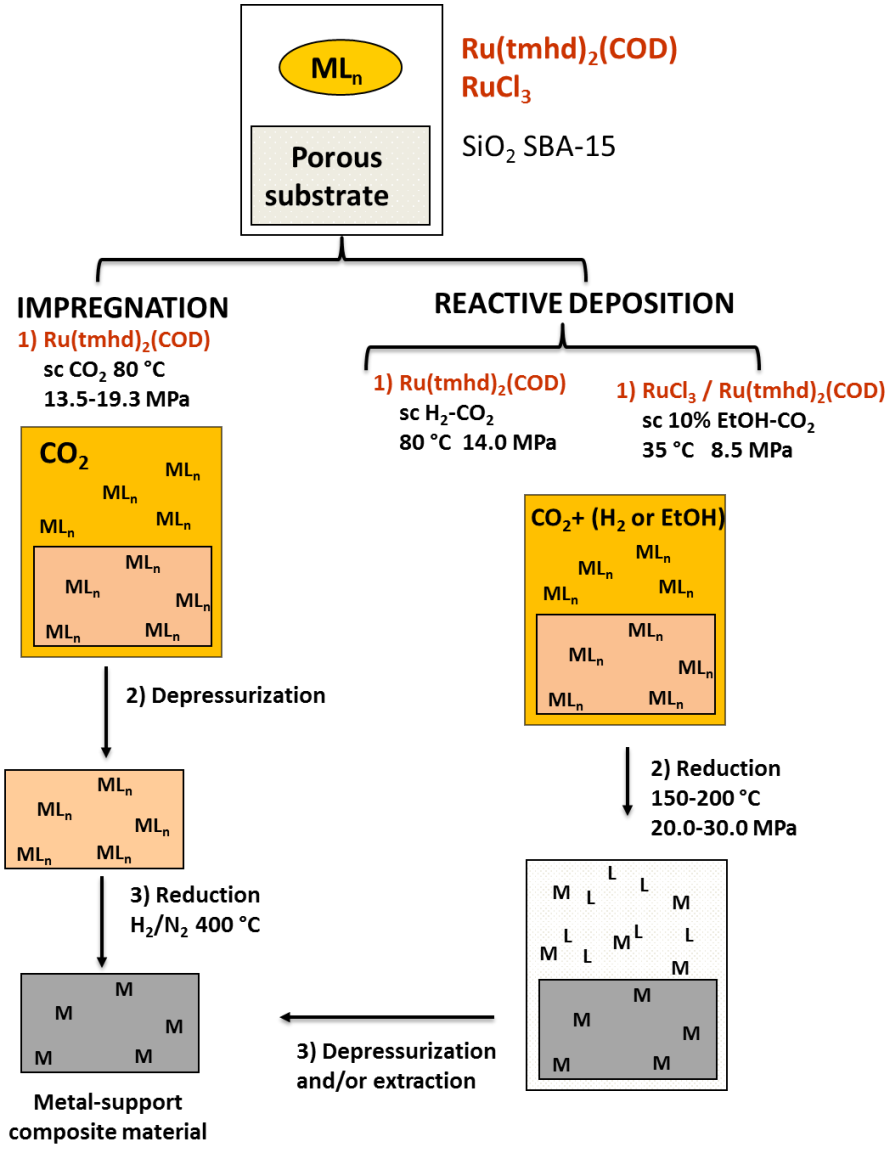

Scheme 1. Summary of the Ru deposition experiments performed by impregnation and reactive deposition using H_2 and EtOH.

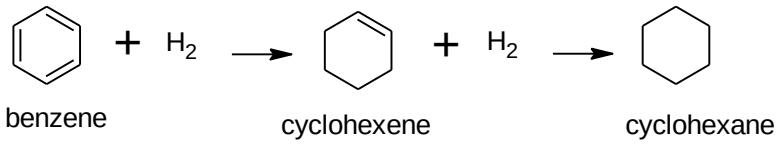

Scheme 2. Reaction pathway for the hydrogenation of benzene.

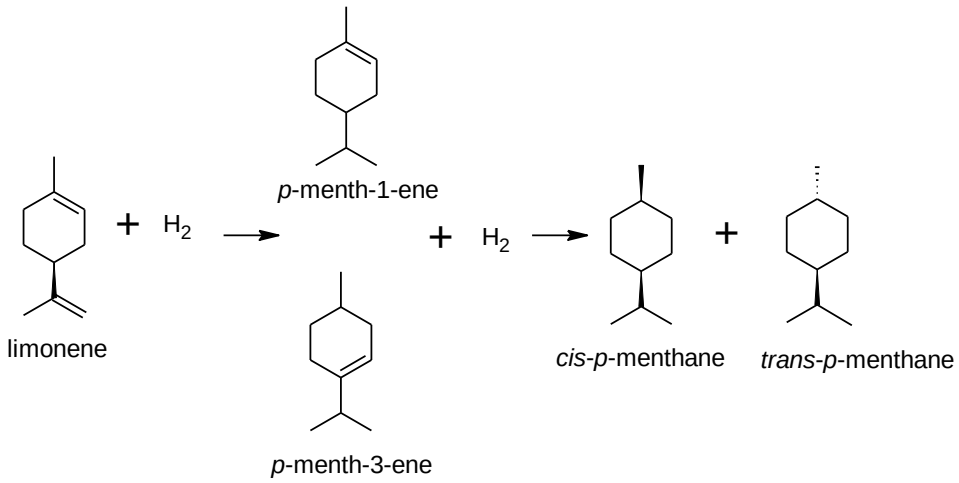

Scheme 3. Main reaction pathway for the hydrogenation of limonene. [58]

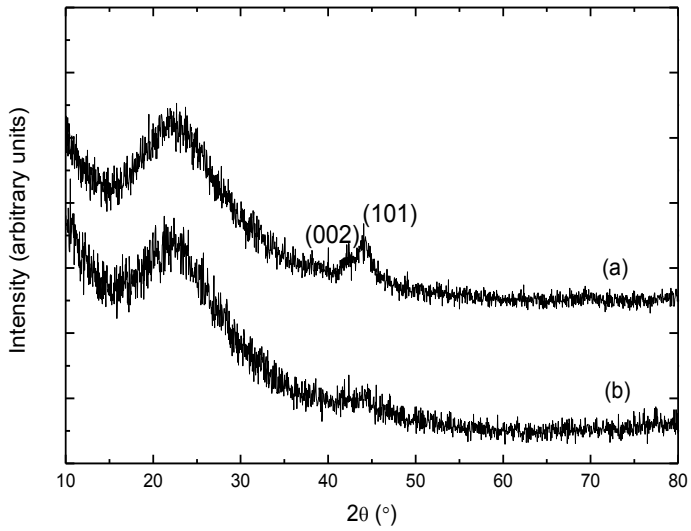

Figure 1. XRD of the Ru/SiO_2 SBA-15 samples obtained by impregnation of $Ru(tmhd)_2(COD)$ in $scCO_2$ at 80ºC and: (a) 13.5 MPa (sample 1) and (b) 19.3 MPa (sample 2), after reduction in H_2/N_2.

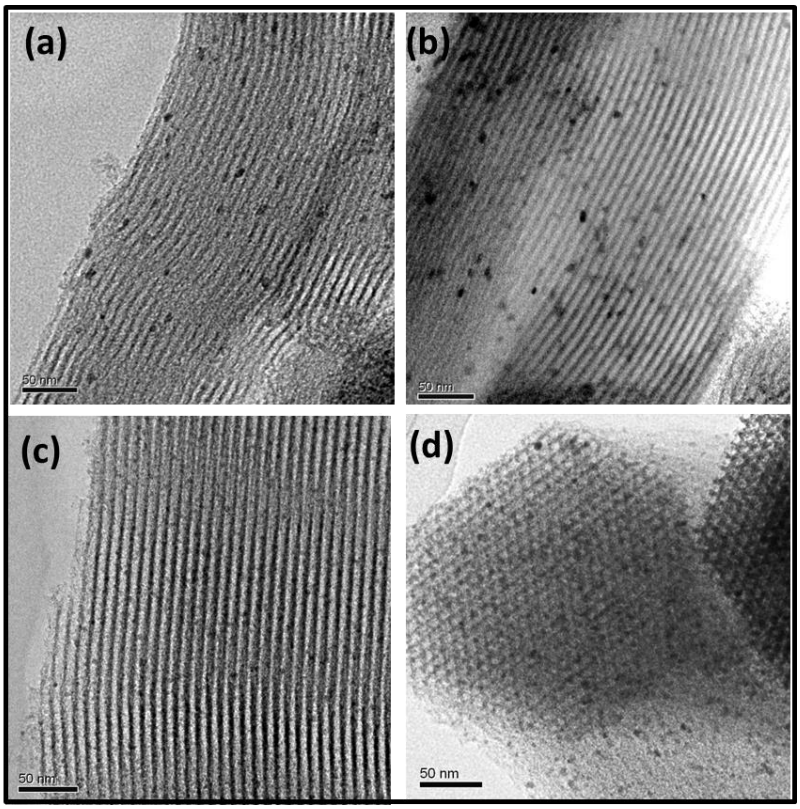

Figure 2. TEM images of Ru/SiO_2 SBA-15 samples obtained by impregnation of $Ru(tmhd)_2(COD)$ in $scCO_2$ at 80ºC and: (a,b) 13.5 MPa (sample 1) and (c, d) 19.3 MPa (sample 2), after reduction in H_2/N_2.

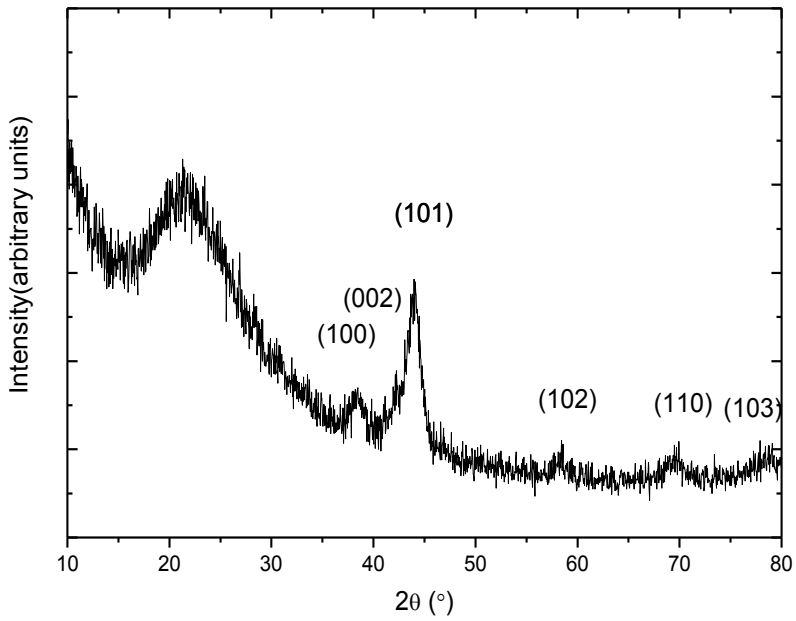

Figure 3. XRD pattern of a Ru/ SiO_2 SBA-15 sample obtained by the H_2-reduction of $Ru(tmhd)_2(COD)$ in $scCO_2$ at 150 ºC (sample 3).

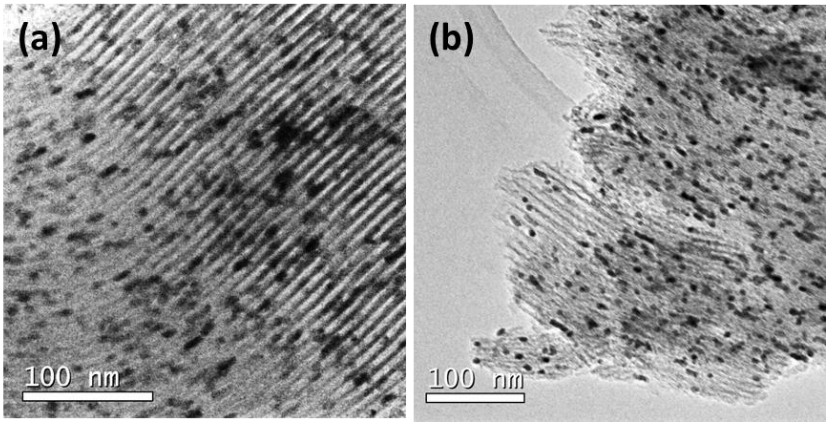

Figure 4. TEM images of a Ru/ SiO_2 SBA-15 sample obtained by the H_2-reduction of $Ru(tmhd)_2(COD)$ in $scCO_2$ at 150 ºC (sample 3).

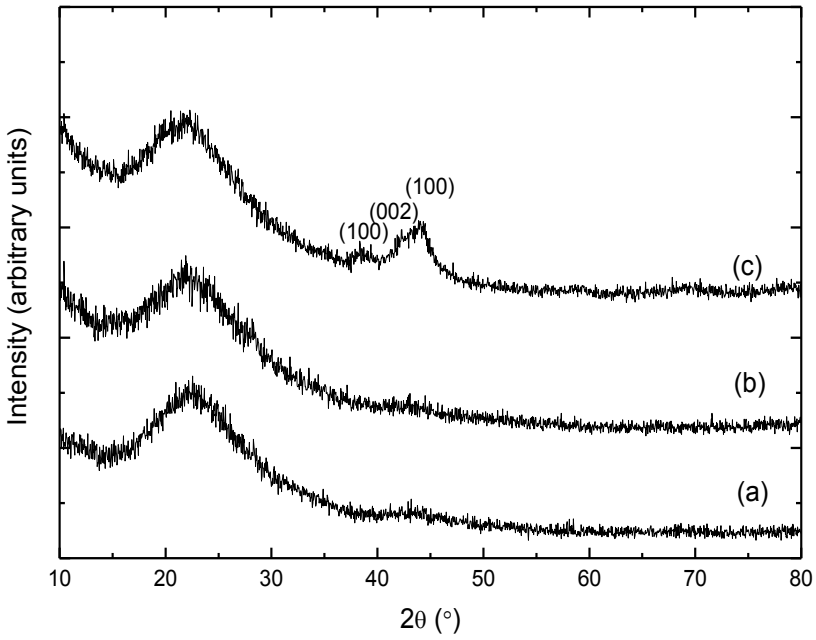

Figure 5. XRD pattern of the Ru/SiO_2 SBA-15 samples obtained by the alcohol reduction of $RuCl_3 \cdot xH_2O$ in $scCO_2$ at different temperatures and/or precursor to support molar ratios: (a) 150 ºC and 1:48 $Ru:SiO_2$ molar ratio (sample 4), (b) 200 ºC and 1:28 $Ru:SiO_2$ molar ratio (sample 5), (c) 150 ºC and 1:6 $Ru:SiO_2$ molar ratio (sample 6).

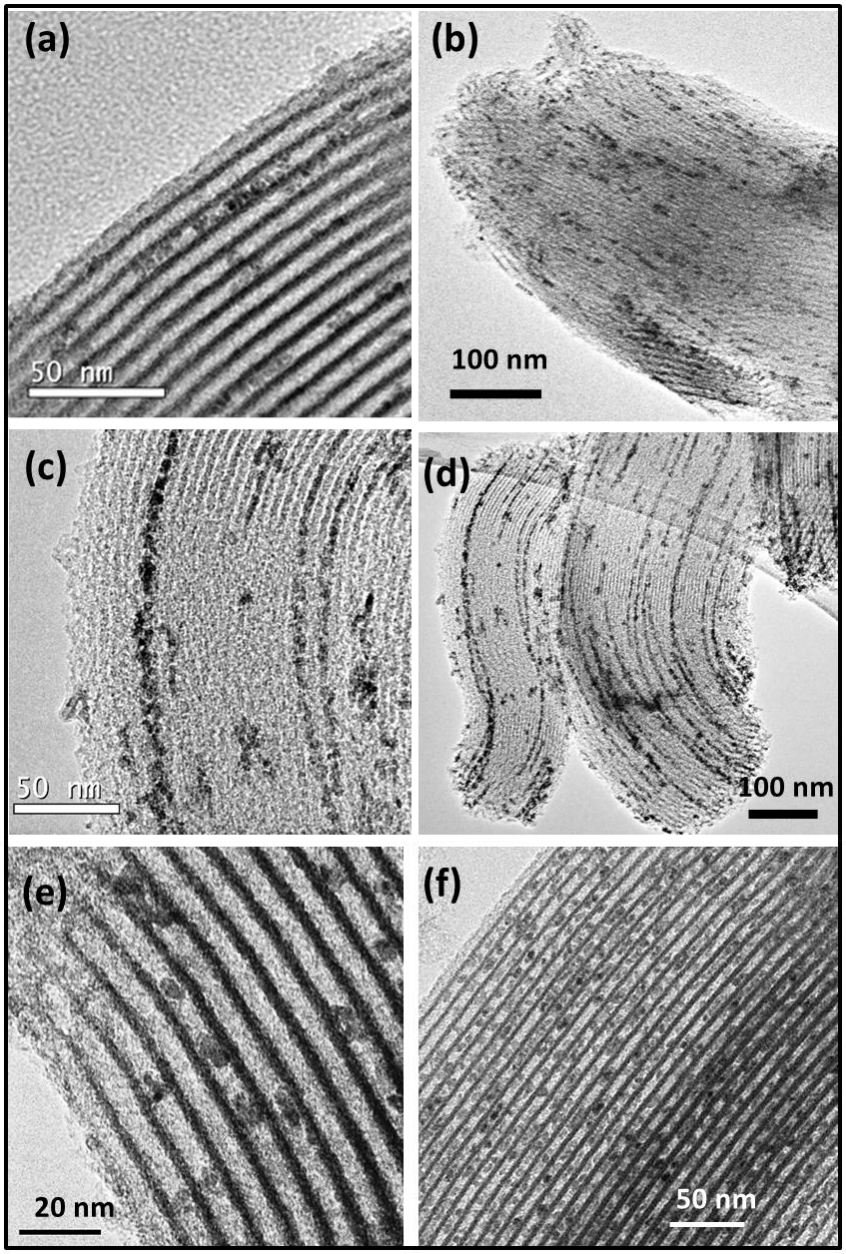

Figure 6. TEM images of the Ru/SiO_2 SBA-15 samples obtained by the alcohol reduction of $RuCl_3 \cdot xH_2O$ in $scCO_2$ at different temperatures and/or precursor to support molar ratios: (a) 150 ºC and 1:48 $Ru:SiO_2$ molar ratio (sample 4), (b) 200 ºC and 1:28 $Ru:SiO_2$ molar ratio (sample 5), (c) 150 ºC and 1:6 $Ru:SiO_2$ molar ratio (sample 6).

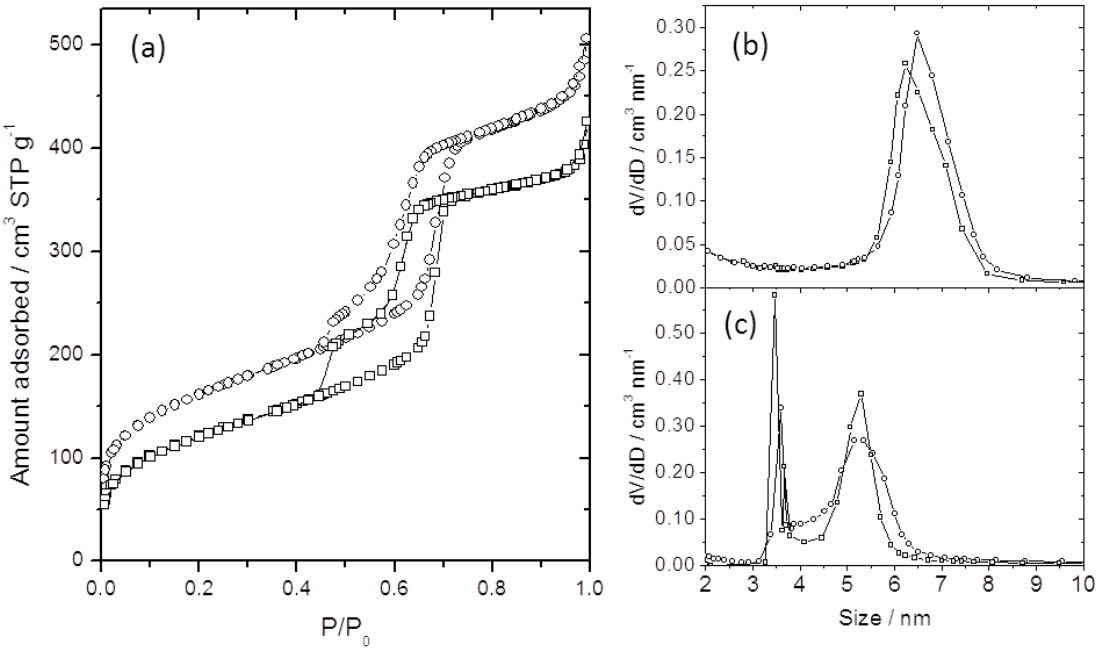

Figure 7. N_2 Adsorption-desorption isotherms (a) and pore size distributions obtained from the adsorption (b) and desorption (c) branches of the isotherm for: (○) Ru/SiO_2 SBA-15 obtained by impregnation of $Ru(tmhd)_2(COD)$ in $scCO_2$ at 80ºC and 13.5 MPa and further reduction in H_2/N_2 (sample 1) and (□) Ru/SiO_2 SBA-15 obtained by H_2-reduction of $Ru(tmhd)_2(COD)$ in $scCO_2$ at 150 ºC (sample 3).

Electronic Supplementary Information (ESI)

Supercritical fluid deposition of Ru nanoparticles into SiO_2 SBA-15 as a sustainable method to prepare selective hydrogenation catalysts

J. Morère[a], M.J. Torralvo[b], C. Pando[a], J.A.R. Renuncio[a] and A. Cabañas*[a]

[a] Department of Physical Chemistry I, Universidad Complutense de Madrid, 28040 Madrid. SPAIN

[b] Department of Inorganic Chemistry I, Universidad Complutense de Madrid, 28040 Madrid. SPAIN

*Send correspondence to:

Prof. Albertina Cabañas

Department of Physical Chemistry I

Universidad Complutense de Madrid

Ciudad Universitaria s/n, 28040 Madrid, SPAIN

Tlf: 34 + 91 3945225 Fax: 34 + 91 3944135

e-mail: a.cabanas@quim.ucm.es

Section S1. Thermogravimetric analysis of the impregnated samples

TGA of the precursor $Ru(tmhd)_2(COD)$, and the SiO_2 support impregnated with $Ru(tmhd)_2(COD)$ at 80ºC and 13.5 MPa (sample 1) and 80ºC and 19.3 MPa (sample 2) in N_2 flow are shown in Figure S1.

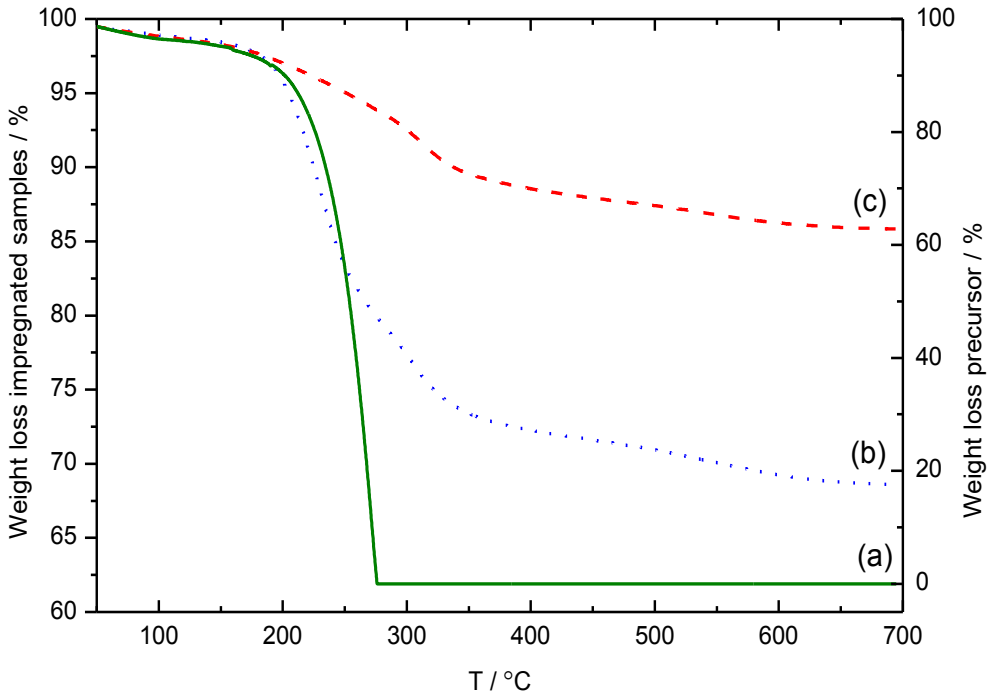

Figure S1. TGA analysis of the precursor $Ru(tmhd)_2(COD)$ (a**,** —) and the SiO_2 SBA-15 support impregnated with $Ru(tmhd)_2(COD)$ at 80ºC and 13.5 MPa (b**,** **…**) and 19.3 MPa (c, ---).

TGA analysis of the precursor $Ru(tmhd)_2(COD)$ showed that this compound sublimes between 200-275 ºC in N_2. However, TGA analysis of a SiO_2 support impregnated with $Ru(tmhd)_2(COD)$ revealed different weight loss events, the first one related to the

sublimation of the precursor adsorbed on SiO_2 at temperatures below 250 ºC. At higher temperatures, the weight loss is associated to the decomposition of the precursor adsorbed onto the surface to its metal form. These results indicate that the hydrophilic SiO_2 support interacts weakly with the precursor and explain that the Ru mol percentage measured by EDX in the impregnated samples after reduction in H_2/N_2 atmosphere is lower than the expected one considering the weight loss by TGA.

Total weight loses close to 30 and 13 mass % were obtained for samples 1 and 2 impregnated at 80 ºC and 13.5 and 19.3 MPa, respectively, at the same Ru:SiO_2 molar ratio. The amount adsorbed decreased as the pressure and density of the supercritical phase increased. At the higher pressure, both the solubility of the precursor in the fluid phase and the concentration of CO_2 increased and consequently, the partition coefficient of the precursor changed, lowering its adsorption on the surface.

Section S2. N_2 adsorption-desorption isotherms

Figures S2 and S3 show N_2 adsorption-desorption isotherms and pore size distributions obtained from the adsorption and desorption branches of the isotherms for the Ru/SiO_2 samples and the bare support not shown in the manuscript.

Isotherms exhibit a type IV, subtype H1, hysteresis loop which is found in mesoporous materials with well-defined cylindrical-like pore channels.

Adsorption isotherms of sample 2 produced by impregnation at 19.3 MPa were very close to those of the SiO_2 support (Figure S2). Due to the small amount of Ru deposited and the small particle size, deposition of Ru by impregnation into the support led to S_{BET} and Vp values very similar to those of the SiO_2 sample.

However, adsorption isotherms of samples 4 to 6 reduced using EtOH showed larger differences in comparison to those of the bare SiO_2 support (Figure S3). This is due in part to the larger amount of Ru deposited for samples 5 and 6, but it is also related to the presence of unreacted $RuCl_3 \cdot xH_2O$ or reaction by-products in the samples deposited using EtOH as determined by EDX. No attempt to correlate the surface area and the pore volume with the concentration and nature of the impurities was made.

Analysis of the pore size distribution of the SiO_2 SBA-15 support obtained from the adsorption branch of the isotherm gave a narrow pore size distribution with a maximum at 6.8 nm. In comparison, there was only a slight reduction of the pore size in all the Ru/SiO_2 samples. The pore size distributions estimated from the desorption branch of the isotherm showed a new maximum at ca. 3.6 nm. This phenomenon is due to ink-bottle like sections

created by the nanoparticles in the mesopores [V. Meynen, et al., Synthesis of siliceous materials with micro- and mesoporosity, Microporous and Mesoporous Materials 104 (2007) 26-38].

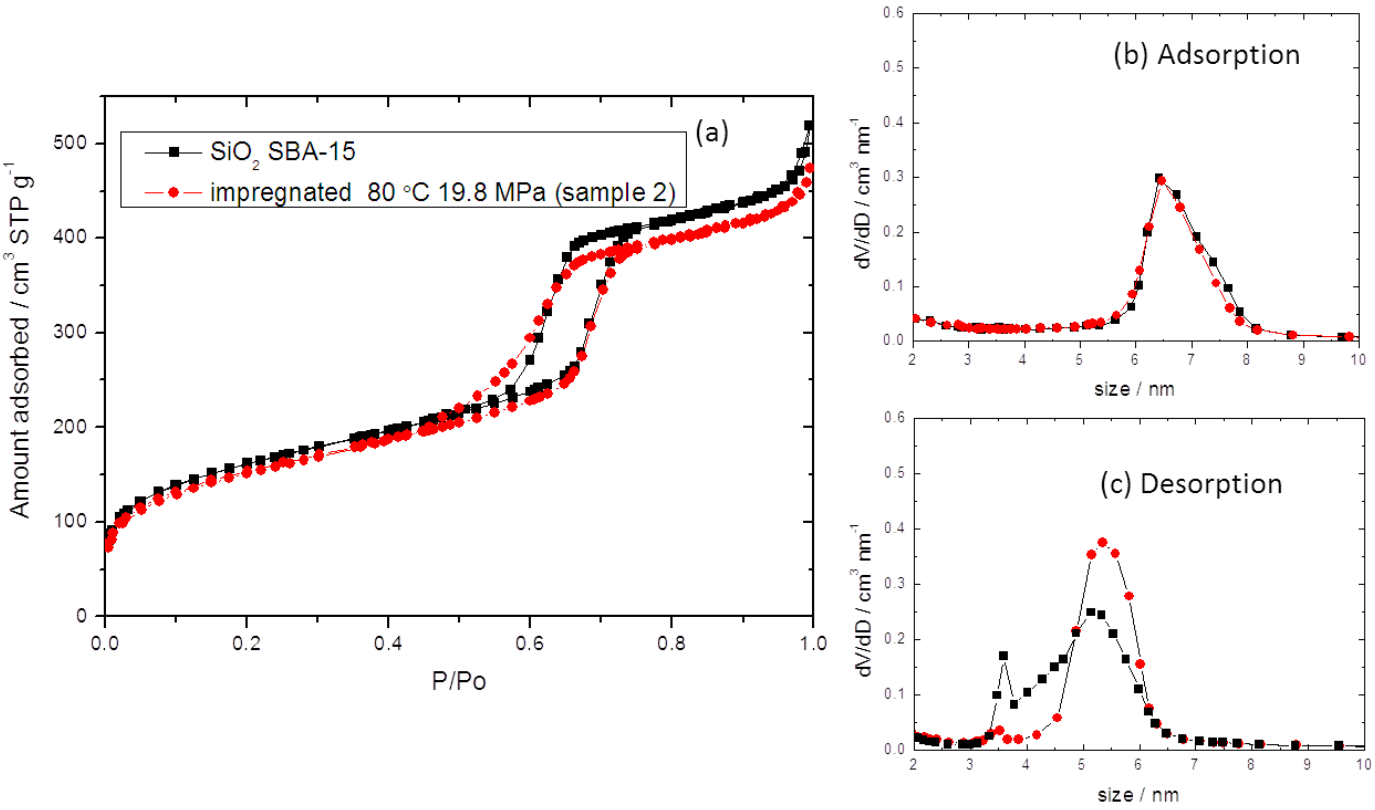

Figure S2. N_2 adsorption-desorption isotherms (a) and pore size distributions obtained from the adsorption (b) and desorption (c) branches of the isotherm for SiO_2 SBA-15 and the Ru/SiO_2 SBA-15 sample obtained by impregnation of $Ru(tmhd)_2(COD)$in $scCO_2$ at 80 ºC and 19.3 MPa (sample 2).

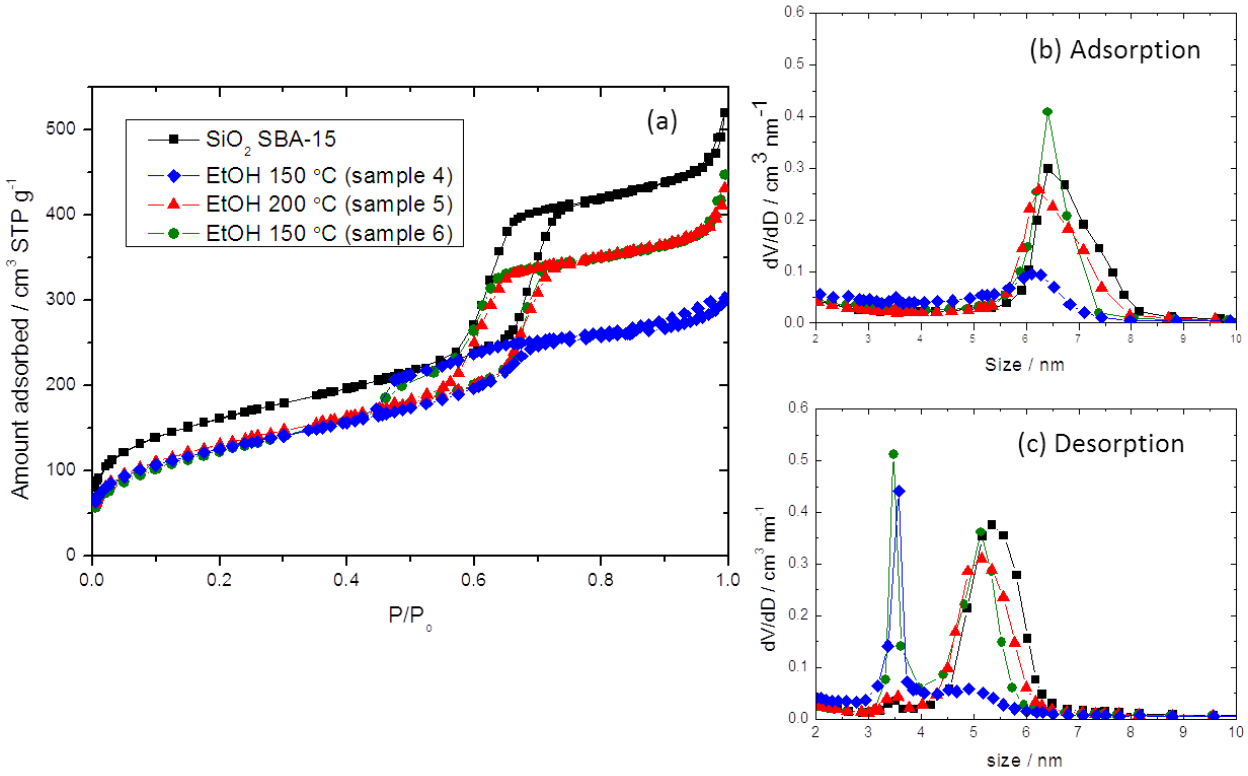

Figure S3. N_2 adsorption-desorption isotherms (a) and pore size distributions obtained from the adsorption (b) and desorption (c) branches of the isotherm for SiO_2 SBA-15 and the Ru/SiO_2 SBA-15 samples obtained by EtOH reduction of $RuCl_3 \cdot xH_2O$ in $scCO_2$ (samples 4-6).